



AIMETA 2003

XVI Congresso AIMETA di Meccanica Teorica e Applicata
16th AIMETA Congress of Theoretical and Applied Mechanics

FERRARA, 9-12 SETTEMBRE 2003

COMITATO ORGANIZZATORE

Claudio ALESSANDRI (Presidente) - *Ferrara*

Antonio TRALLI (Vicepresidente) - *Ferrara*

Vincenzo MALLARDO - *Ferrara*

Domenico CAPUANI - *Ferrara*

Gianni ROYER CARFAGNI - *Parma*

Vincenzo COSCIA - *Ferrara*

Alessandro VALIANI - *Ferrara*

Carlo CINQUINI - *Pavia*

Antonio STROZZI - *Modena-Reggio Emilia*

Lucio NOBILE - *Bologna*

Giorgio DAL PIAZ - *Ferrara*

COMITATO SCIENTIFICO

Gian Antonio SACCHI LANDRIANI (Presidente) - *Milano*

Guido BURESTI - *Pisa*

Roberto CONTRO - *Milano*

Vincenzo D'AGOSTINO - *Salerno*

Gianpiero DEL PIERO - *Ferrara*

Carlo GALLETTI - *Genova*

Giorgio GRAZIANI - *Roma*

Giuseppe MUSCOLINO - *Messina*

Franco PASTRONE - *Torino*

Umberto PEREGO - *Milano*

Furio VATTA - *Torino*

CONSIGLIO DIRETTIVO AIMETA

Giuliano AUGUSTI (Vicepresidente) - *Roma*

Maurizio PANDOLFI (Tesoriere) - *Torino*

Carlo CINQUINI (Segretario) - *Pavia*

Angelo MORRO (Presidente) - *Genova*

Gianfranco CAPRIZ (Past-president) - *Pisa*

Roberto BASSANI - *Pisa*

Mario DI PAOLA - *Palermo*

SO Sessioni Ordinarie

GEN Meccanica Generale
FLU Meccanica dei Fluidi
MAC Meccanica delle Macchine
SOL Meccanica dei Solidi
STR Meccanica delle Strutture

SS Sessioni Speciali

MECOM Meccanica Computazionale
INV Problemi Inversi nella Meccanica dei Materiali e delle
 Strutture
DSM Dinamica dei sistemi Meccanici, Dinamica Lineare e
 Nonlineare, Controllo e Risposta Strutturale
MEP Microstrutture in Elasticità e Plasticità
COMP Problemi di Frattura e Problemi di Interfaccia nei Materiali
 Compositi
SSI Strutture Sottili Insolite

A MECHANICAL MODEL FOR DELAMINATION GROWTH UNDER CYCLIC COMPRESSION

P. S. VALVO¹ and S. BENNATI¹

¹ *Dipartimento di Ingegneria Strutturale, Università di Pisa, Pisa*

SOMMARIO

La memoria illustra un modello meccanico capace di descrivere la crescita per fatica di delaminazioni promossa da instabilità locale in laminati compositi soggetti a carichi ciclici di compressione. Il laminato è visto come l'unione di due sublaminati parzialmente collegati da un'interfaccia elastica, a sua volta modellata attraverso un letto di molle elasto-fragili, agenti sia nella direzione normale che in quella tangente al piano dell'interfaccia.

Il modello consente di determinare le espressioni esplicite delle componenti normale e tangenziale degli sforzi interlaminari e dei loro valori di picco sul fronte della delaminazione; quindi, consente di valutare separatamente i contributi dei modi I e II alla velocità di rilascio dell'energia potenziale totale e l'angolo di modo misto. Sulla base di tali risultati, è possibile utilizzare una legge di crescita per fatica che tenga conto della presenza contemporanea di diversi modi di propagazione della frattura, determinando, per ogni valore del carico, il numero di cicli necessari per far estendere la delaminazione fino ad una lunghezza assegnata. I risultati evidenziano modalità di crisi particolarmente insidiose e sembrano contribuire a spiegare alcuni fenomeni di propagazione instabile e di arresto osservati sperimentalmente.

ABSTRACT

The paper illustrates a mechanical model for describing the fatigue-driven, mixed-mode delamination growth fostered by local instability phenomena in composite laminates subjected to cyclic compressive loads. The laminate is modelled as the union of two sublaminates partly bonded together by an elastic interface, in turn, represented by a continuous array of linear elastic springs acting in directions normal and tangential to the interface plane.

The model allows for determining the explicit expressions for the normal and tangential interlaminar stresses exerted between the sublaminates at the delamination front, as well as their peak values. It thus enables evaluating the individual contributions of modes I and II to the potential energy release rate as well as the value of the mode-mixity angle. Based on the results obtained, a mode-dependent fatigue growth law can then be applied to take into account the simultaneous actions of the two different crack propagation modes. Thus, for any load level, predictions can be made on the number of cycles needed for a delamination to extend to a given length. The results shed light on the mechanisms underlying some very insidious failures and seem able to help explain some experimentally observed phenomena of delamination growth and arrest.

1. INTRODUCTION

Delamination can arise in fibre-reinforced composite laminates as the result of many common events, such as manufacturing errors or low-velocity impacts [1, 2, 3]. When a laminated plate containing a delamination is loaded under compression, instability phenomena may promote further crack growth and, in some cases, lead to failure [4, 5, 6]. In order to model the process, the loss of stability can be studied through the methods of non-linear structural analysis, while delamination growth can be described through typical fracture mechanics. In earlier studies, the total potential energy release rate, G , was taken to be the parameter indicating the onset of crack growth [7]. However, experimental studies on the subject have shown that crack growth almost always involves the three classical modes of crack propagation: opening, sliding and tearing. Therefore, delamination growth is more properly described by using a mixed-mode growth criterion, whose application requires the energy release rate to be broken up into the sum of the contributions G_I , G_{II} and G_{III} , corresponding to the three propagation modes. To this end, the peak values of the interlaminar stresses at the crack-tip, responsible for delamination growth, need to be evaluated [8, 9].

Previous works by the authors [10, 11, 12] introduced a mechanical model for a delaminated plate subjected to monotonic compression. The plate is modelled as the union of two sublaminates, partly bonded together by an elastic interface, which is in turn represented by a continuous array of linear elastic springs acting in directions normal and tangential to the interface plane [13, 14, 15, 16]. The model allows for the determining the explicit expressions for the normal and tangential interlaminar stresses exerted between the sublaminates at the delamination front, as well as their peak values. It thus furnishes the individual contributions of modes I and II to the energy release rate, as well as the mode-mixity angle. Finally, a mixed-mode growth criterion can be applied in order to predict the phenomena of delamination buckling and growth under static compressive loads.

The present paper extends the model outlined in the foregoing to include the case of delamination growth under cyclic compressive loads. In such cases, as the delaminated plate undergoes repeated buckling and unloading, damage is progressively accumulated at the delamination front. As a consequence, an existing delamination may grow, even if the static growth criterion is not satisfied (i.e., if the energy release rate is less than the critical value). In what follows, a fatigue growth law, based on a mode-dependent critical energy release rate, is applied [17]. This enables predicting the number of cycles needed for a delamination to grow to a given length. The results shed light on the mechanisms underlying some very insidious failures and seem able to help explain some experimentally observed phenomena of delamination growth and arrest.

2. THE ELASTIC INTERFACE MODEL

Let us consider a rectangular laminated plate of length $2L$, width B , and thickness H , affected by a central, through-the-width delamination of length $2a$. The laminate is subjected to two compressive loads of intensity P acting in the axial direction. The material is assumed to be homogeneous and linearly elastic, with orthotropy axes aligned with those of the global reference system $OXYZ$.

The elastic interface model (Fig. 1) conceives of the delaminated plate as the union of two sublaminates, partly bonded by a continuous array of linear elastic springs. The two individual sublaminates are referred to as the ‘film’, which is the layer between the delamination plane

and the nearest external surface (thickness H_f), and the ‘substrate’ (thickness $H_s = H - H_f$). The interface springs act in both the normal and tangential directions to the interface plane, where they are characterized by the elastic constants, k_z and k_x , respectively. The width B is assumed to be ‘very large’, so the sublaminates can be modelled as beam-plates. Hence, the ‘reduced’ Young modulus $E_X^* = E_X / (1 - \nu_{XZ} \nu_{ZX})$ is introduced, and all calculations refer to a unit width. According to the classical laminated plate theory, $A_f = E_X^* H_f$ and $D_f = E_X^* H_f^3 / 12$ are the extensional and bending stiffness of the film, respectively; $A_s = E_X^* H_s$ and $D_s = E_X^* H_s^3 / 12$ are those of the substrate, and $A = E_X^* H$ and $D = E_X^* H^3 / 12$ are those of the base laminate.

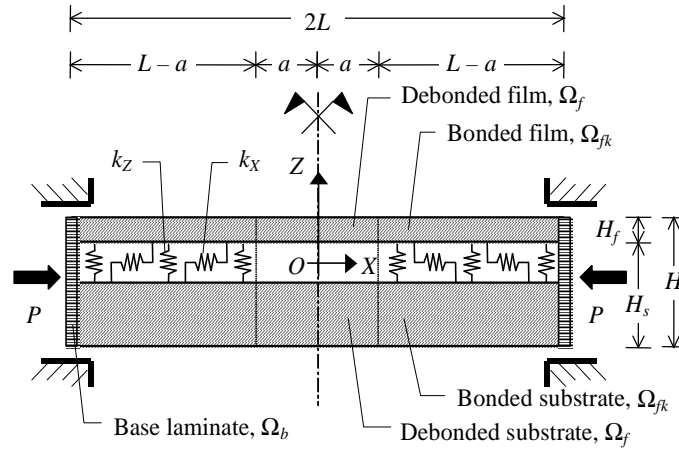


Fig. 1: The elastic interface model

Under these assumptions, the differential equations of the equilibrium problem according to von Kármán’s plate theory have been derived and solved completely in closed form. The explicit expressions for the solution in the pre- and post-buckling phases are reported in the above-cited works [10, 11, 12]. Herein, we limit ourselves to recalling the fundamental results.

The pre-buckling phase is characterized by a linear relationship between the applied load, P , and the end displacement of the plate, u . During this phase, the sublaminates undergo uniform shortening, and the axial force is distributed between them in proportion to their extensional stiffness. This behaviour ceases when the axial force in the debonded film, Ω_f , equals the buckling load of the subl laminate. This is determined by numerically solving a non-linear transcendental equation, which yields the buckling load of the delaminated plate, P_B , i.e., the load applied to the base laminate at the incipient buckling of the film.

During the post-buckling phase, the substrate experiences axial shortening alone, while the film undergoes bending as well as shortening. Because of the different displacements of the two laminates, non-zero stresses arise in the interface springs. Moreover, the energy release rate, $G = -\partial\Pi/\partial a$ (Π is the total potential energy of the system), which is zero throughout the pre-buckling phase, starts to increase.

G is the sum of the contributions of mode I and II:

$$G = G_I + G_{II} \quad (1)$$

which are:

$$G_I = \frac{k_z a_{fk}^2}{2} \frac{8\lambda}{\frac{2a}{\lambda} - \sin\left(\frac{2a}{\lambda}\right)} \left(a + \omega \tanh \frac{L-a}{\omega} \right) \frac{P - P_B}{A_s} \quad (2a)$$

$$G_{II} = \frac{k_x}{2} \left(\omega \tanh \frac{L-a}{\omega} \frac{P - P_B}{A_s} \right)^2 \quad (2b)$$

where $\lambda^2 = (A D_f) / (A_f P_B)$; $\omega^2 = [k_x (A_f^{-1} + A_s^{-1})]^{-1}$; and a_{fk} is a dimensionless integration constant.

Finally, the mode-mixity angle,

$$\psi = \arctan \sqrt{\frac{k_x G_{II}}{k_z G_I}} \quad (3)$$

is deduced. By convention, this provides a measure of the relative amount of fracture modes through values ranging from 0° (pure mode I) to 90° (pure mode II).

3. STATIC DELAMINATION GROWTH

According to Griffith's classical criterion, crack growth is to be expected when G equals a critical value, G_C . In the original and simplest formulation, G_C is a material constant, measuring the so-called 'toughness'. Nevertheless, for anisotropic materials such as composite laminates, experimental determinations of G_C are markedly dependent on the propagation mode acting in the test performed (I or opening, II or sliding, III or tearing). Actually, the critical value measured in pure mode III tests, $G_{III C}$, is usually greater than that obtained in pure mode II tests, $G_{II C}$, which may, in turn, be much greater than the value measured in pure mode I tests, $G_{I C}$.

Under mixed-mode conditions, as all propagation modes are simultaneously active, the toughness equals an intermediate value. Thus, in order to predict crack growth, a mixed-mode criterion is to be adopted, by which G_C is considered to be a function of the relative amount of the different propagation modes. In particular, for plane problems, the critical energy release rate,

$$G_C(\psi) = \frac{G_{I C}}{1 + (\gamma - 1) \sin^2(\psi)} \quad (4)$$

where $\gamma = G_{I C} / G_{II C}$, may be conveniently defined as a function of the mode-mixity angle [9].

For the present model the energy release rate, G , in the post-buckling phase is an increasing function of the applied load, P , as shown by equations (1) and (2). Moreover, the mode-mixity angle, ψ , increases as either the load or the delamination length grows. For any assigned delamination length, it is possible to determine the load, $P_G(a)$, at which $G = G_C(\psi)$, and static delamination growth is expected. Fig. 2 shows the buckling load of the delaminated plate, P_B , and the static delamination growth load, P_G , as functions of the delamination half-length, a . The following numerical values have been adopted: $L = 100$ mm, $H = 10$ mm and $H_f = 1$ mm;

$E_X = 54$ GPa and $\nu_{XZ} = 0.25$; $k_X = 17284$ N/mm³ and $k_Z = 23333$ N/mm³; $G_{IC} = 100$ J/m² and $G_{II C} = 1000$ J/m². The loads have been divided by the Euler load, $P_{eul} = \pi^2 D / L^2 = 4535.8$ N/mm, and the delamination half-length has been divided by L .

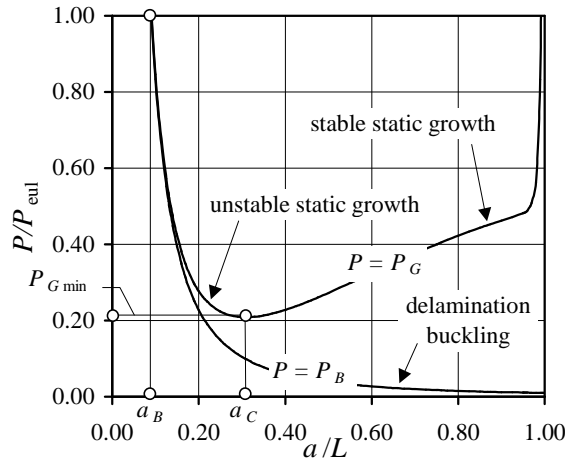


Fig. 2: Buckling load and static delamination growth load vs. delamination half-length

Two significant values of the delamination half-length have been highlighted in the figure: a_B , at which $P_B = P_{eul}$, and a_C , at which P_G reaches a local minimum, P_{Gmin} . If the length of the existing delamination is such that $a < a_B$, then local buckling phenomena and related delamination growth are not to be expected (although global instability can obviously occur); if, on the other hand, $a_B < a < a_C$, then delamination buckling and growth will be possible, the latter resulting in an unstable process; finally, if $a_C < a$, then delamination buckling and growth will be possible, though as a stable process.

For what follows it is useful to introduce an equivalent alternative formulation of the growth criterion. To this end, the energy release rate is normalized with respect to the mode-dependent toughness:

$$\hat{G} = \frac{G}{G_c(\psi)} \quad (5)$$

Consequently, under static loading, the condition for delamination growth becomes $\hat{G} = 1$, while no growth is instead predicted for $\hat{G} < 1$. With reference to Fig. 2, the static growth condition is fulfilled by points belonging to the 'growth curve', $P = P_G$. On the other hand, points located below or on the 'buckling curve', $P = P_B$, furnish $\hat{G} = 0$. Lastly, for all points in the region between the above two curves, $0 < \hat{G} < 1$, no static growth is expected. However, delamination growth under cyclic loads is possible, as explained in the next paragraph. Finally, we should also note that \hat{G} turns out to be greater than 1 for all points located above the growth curve. This means that these points are not reachable via a quasi-static load history. Therefore, they have no meaning within the present model, which does not account for any dynamic effects.

4. FATIGUE DELAMINATION GROWTH

Moving on to examine the case of fatigue delamination growth, let us consider a laminated plate affected by a delamination whose initial half-length is a_0 . We assume that the applied compressive load varies cyclically between P_{\min} and P_{\max} , so that the energy release rate will vary between G_{\min} and G_{\max} . In these cases, experimental studies show that delamination growth can occur because of the progressive accumulation of damage at the delamination front as the delaminated plate undergoes repeated buckling and unloading.

According to [17], a fatigue growth law can be postulated,

$$\frac{da}{dN} = c(\psi) \frac{(\Delta \hat{G})^{m(\psi)}}{1 - \hat{G}_{\max}} \quad (6)$$

where N is the number of load cycles performed, and

$$\Delta \hat{G} = \frac{G_{\max} - G_{\min}}{G_c(\psi)} \quad (7)$$

is the range of the normalized energy release rate. In turn, $c(\psi)$ and $m(\psi)$ are two mode-dependent parameters to be determined by experiment. In particular, the multiplicative factor is

$$c(\psi) = c_I [1 + (\kappa - 1) \sin^2(\psi)] \quad (8)$$

where $\kappa = c_{II} / c_I$; c_I and c_{II} are the values measured in pure mode I and II tests, respectively. Analogously, mode dependence is introduced for the exponent, by setting

$$m(\psi) = m_I [1 + (\mu - 1) \sin^2(\psi)] \quad (9)$$

where $\mu = m_{II} / m_I$; m_I and m_{II} are the values measured in pure mode I and II tests, respectively. The numerical values used for all subsequent figures are: $c_I = 50$ mm/cycle and $\kappa = 10$; $m_I = 10$ and $\mu = 0.50$.

In what follows we will assume that cycles are performed with $G_{\min} = 0$, so that $\Delta \hat{G} = \hat{G}_{\max}$, and the fatigue growth rate (6) becomes:

$$\frac{da}{dN} = c(\psi) \frac{(\hat{G}_{\max})^{m(\psi)}}{1 - \hat{G}_{\max}} \quad (10)$$

This assumption, however, does not necessarily imply $P_{\min} = 0$, but just that $P_{\min} \leq P_B$, since $G = 0$ in the pre-buckling phase.

The fatigue growth rate, da/dN , is a positive increasing function of \hat{G}_{\max} . Moreover, because of the denominator of equation (10), as \hat{G}_{\max} approaches unity, the growth rate goes to infinity, so that instant (static) growth is predicted (Fig. 3a). Also, da/dN is an increasing function of ψ (Fig. 3b). Therefore, since the mode-mixity angle increases as the delamination

grows longer [12], the growth rate is expected to become higher and higher as the process of fatigue growth itself develops.

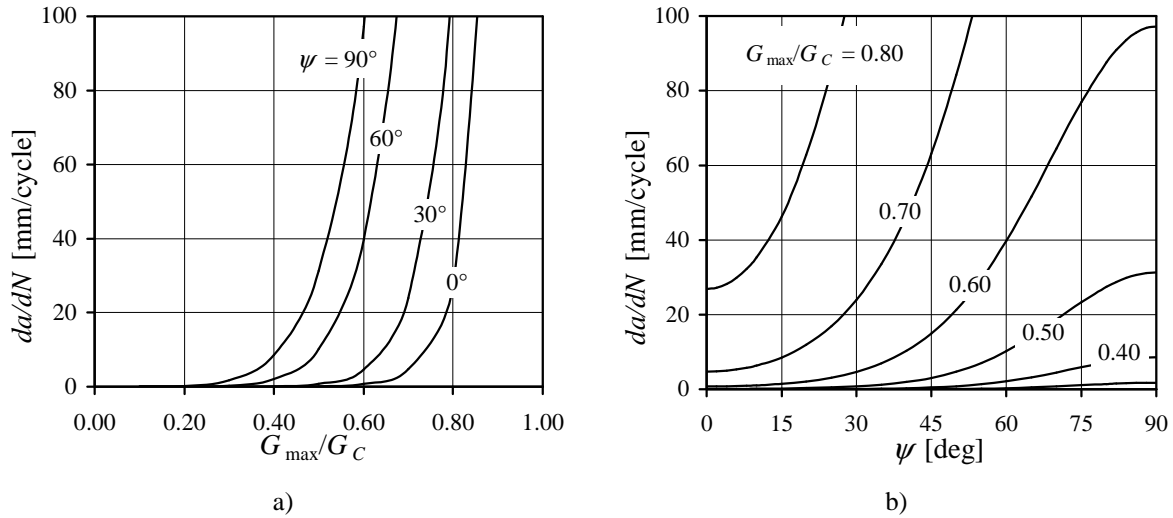


Fig. 3: Fatigue growth rate: a) vs. normalized energy release rate and b) vs. mode-mixity angle

Fig. 4a shows \hat{G}_{max} as a function of the delamination half-length. The dashed curve is for $P_{max} = P_{Gmin}$: at this load level, \hat{G}_{max} presents a local maximum equal to 1. The curves below the dashed one are for $P_{max} < P_{Gmin}$: here it is always $\hat{G}_{max} < 1$. Finally, the curves above the dashed one are for $P_{max} > P_{Gmin}$: at these load levels, some values of \hat{G}_{max} are greater than unity and must therefore be excluded.

Fig. 4b represents da/dN as a function of the delamination half-length. Once again, the dashed curve is for $P_{max} = P_{Gmin}$: for this and all higher load values, da/dN presents a vertical asymptote. Instead, for $P_{max} < P_{Gmin}$, the curves have a local maximum.

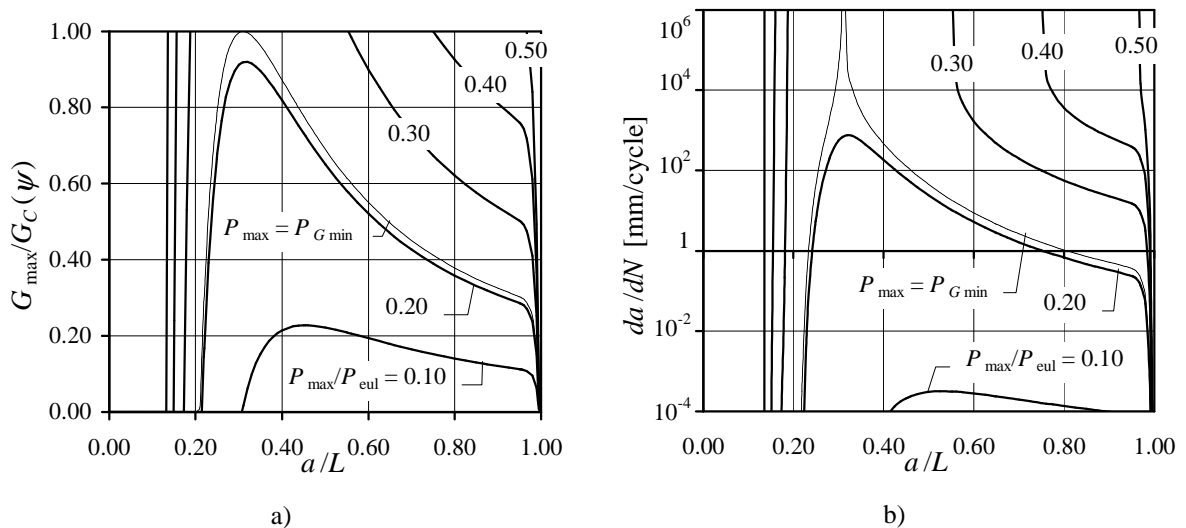


Fig. 4: a) Normalized energy release rate and b) Fatigue growth rate vs. delamination half-length

The number of cycles needed for the delamination to grow from its initial length, $2a_0$, to a current length, $2a$, is given by:

$$\Delta N(a_0, a) = \int_{a_0}^a \frac{dN}{d\bar{a}} d\bar{a} = \int_{a_0}^a \frac{1}{c(\psi)} \frac{1 - \hat{G}_{\max}}{(\hat{G}_{\max})^{m(\psi)}} d\bar{a}. \quad (11)$$

Because of the analytical complexity of equation (11), the integration must be carried out numerically. In the following, two cases are considered separately.

When the maximum load, P_{\max} , is less than the minimum load at which static growth can occur, $P_{G\min} = P_G(a_C)$, then the straight line, $P = P_{\max}$, intersects the buckling curve, $P = P_B$, at one point where the delamination half-length, a_F , is such that $P_B(a_F) = P_{\max}$ (Fig. 5a). If the initial delamination length is such that $a_0 \leq a_F$, then no fatigue growth is expected, since no local buckling will take place; instead, if $a_0 > a_F$, then fatigue growth is predicted. Moreover, fatigue growth will be ‘unlimited’, since in theory it can continue until the plate is completely delaminated.

Instead, when the maximum load, P_{\max} , is greater than the minimum static growth load, $P_{G\min}$, then the straight line, $P = P_{\max}$, intersects the buckling curve, $P = P_B$, at a_F . It also intersects the growth curve, $P = P_G$, at two points where the delamination half-length is, respectively, a_{G1} and a_{G2} (Fig. 5b). As in the previous case, if the initial delamination length is such that $a_0 \leq a_F$, then no fatigue growth is expected since no buckling will occur. Likewise, if $a_0 > a_{G2}$, then ‘unlimited’ fatigue growth will take place. Instead, different behaviour emerges in the range of $a_F < a_0 < a_{G1}$: here, fatigue growth is possible, though it will be ‘limited’. In fact, after a finite number of cycles have completed, at $a = a_{G1}$, the conditions for static growth are fulfilled and the process can possibly continue in the form of static growth until $a = a_{G2}$.

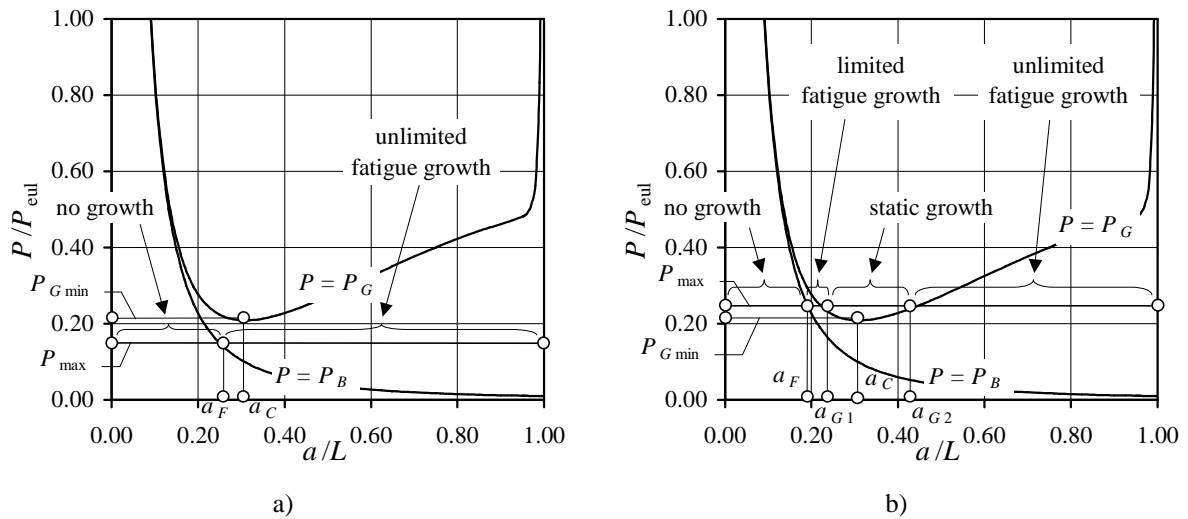


Fig. 5: Fatigue delamination growth: a) $P_{\max} \leq P_{G\min}$ and b) $P_{\max} > P_{G\min}$

The following two figures are for $P_{\max} \leq P_{G\min}$. They show the delamination half-length as a function of the number of load cycles. A dashed line marks the value, a_F , for which no fatigue growth occurs. Depending upon the maximum load level, the qualitative trend of the fatigue growth process changes considerably. In Fig. 6a, the load level is quite low ($P_{\max}/P_{eul} = 0.10$), and the delamination does not increase appreciably in length until more than 10^4 cycles have been performed. In Fig. 6b, the maximum load ($P_{\max}/P_{eul} = 0.20$) is very close to the minimum static growth load ($P_{G\min}/P_{eul} = 0.2084$): here, rapid fatigue growth takes place, leading to complete delamination in a number of load cycles of less than 10^2 .

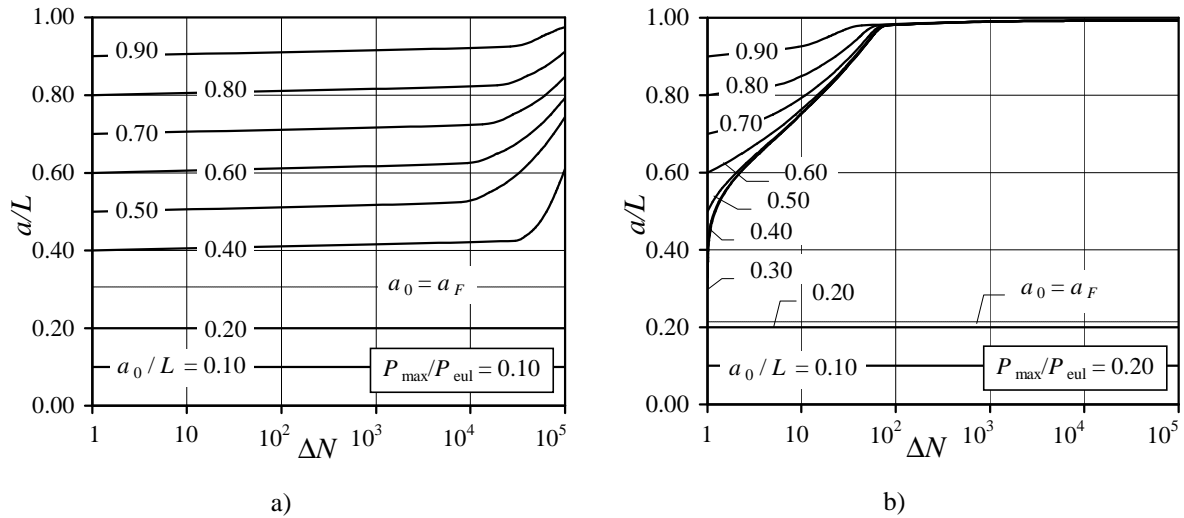


Fig. 6: Delamination half-length vs. number of load cycles at constant maximum load:
a) $P_{\max} = 0.10 P_{eul}$ and b) $P_{\max} = 0.20 P_{eul}$

The last plot (Fig. 7) is for $P_{\max} > P_{Gmin}$. It shows the delamination half-length as a function of the number of load cycles. For $a_0 > a_{G2}$, very rapid fatigue growth is expected, leading to complete delamination in less than 10 cycles. The curve for $a_0 = 0.20$ (in the ‘limited’ fatigue growth range) predicts peculiar behaviour, by which the delamination begins to grow very slowly, then, at $a = a_{G2}$, it suddenly makes a ‘jump’ leading to complete delamination. Such behaviour clearly represents a very insidious and dangerous failure mode.

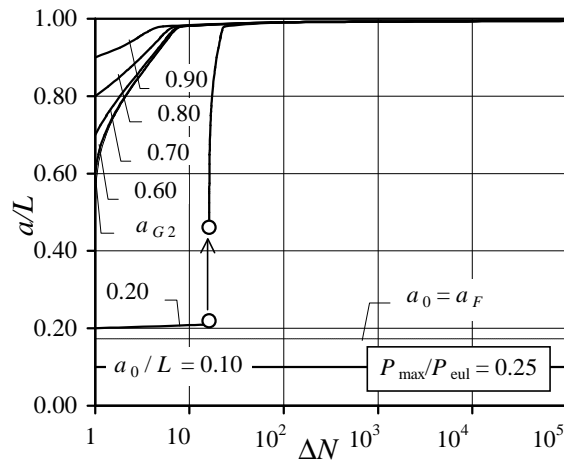


Fig. 7: Delamination half-length vs. number of load cycles at constant maximum load: $P_{\max} = 0.25 P_{eul}$

5. CONCLUSION

The proposed mechanical model allows for deducing the explicit expressions for the normal and tangential interlaminar stresses at the delamination front, when local instability phenomena are present. Thus, it also allows for determining the oscillation in intensity of the crack-growth forces, when cyclic compressive loads are acting.

Once a suitable fatigue delamination growth criterion has been chosen, it is possible to follow the evolution of the delaminated area. The results show that small changes in the

governing parameters (initial delamination length, intensity of the maximum load) are sufficient to produce totally different growth paths. These appear to be characterised by either a very slow evolution even for a very high number of cycles, or by a sudden transition in the growth mechanism and by the arising of a nearly unstable growth.

REFERENCES

- [1] Garg A. C.: Delamination – A damage mode in composite structures, *Engineering Fracture Mechanics*, Vol. 29, pp. 557-584 (1988).
- [2] Abrate S.: Impact on laminated composite materials, *Appl. Mech. Reviews*, Vol. 44, pp. 155-190 (1991).
- [3] Bolotin V. V.: Delaminations in composite structures: its origin, buckling, growth and stability, *Composites Part B: Engineering*, Vol. 27, pp. 129-145 (1996).
- [4] Kachanov L. M., *Delamination buckling of composite materials*; Kluwer Academic Publishers, Dordrecht-Boston-London, 1988.
- [5] Storåkers B.: Nonlinear aspects of delamination in structural members; *ICTAM '89, 17th International Congress of Theoretical and Applied Mechanics*, Grenoble, France, 1988; Proceedings, pp. 315-336, North-Holland, Elsevier Science Publishers, Amsterdam, 1989.
- [6] Chai H., Babcock C. D., Knauss W. G.: One dimensional modelling of failure in laminated plates by delamination buckling, *Int. J. of Solids and Structures*, Vol. 17, pp. 1069-1083 (1981).
- [7] Yin W.-L., Wang, J. T.-S.: The energy-release rate in the growth of a one-dimensional delamination, *Trans. ASME, J. of Applied Mechanics*, Vol. 51, pp. 939-941 (1984).
- [8] Whitcomb J. D.: Finite element analysis of instability related delamination growth, *J. of Composite Materials*, Vol. 15, pp. 403-426 (1981).
- [9] Hutchinson J. W., Suo Z.: Mixed mode cracking in layered materials, *Advances in Applied Mechanics*, Vol. 29, pp. 63-191 (1992).
- [10] Valvo P. S.: Fenomeni di instabilità e di crescita della delaminazione nei laminati compositi; Tesi di Dottorato, Università degli Studi di Firenze, 2000.
- [11] Bennati S., Valvo P. S.: An elastic-interface model for delamination buckling in laminated plates; *5th Seminar on Experimental Techniques and Design in Composite Materials*, Cagliari, Italy, September 28-29, 2000; Proceedings, *Key Engineering Materials*, Vol. 221-222, pp. 293-306 (2002).
- [12] Bennati S., Valvo P. S.: A mechanical model for mixed-mode buckling-driven delamination growth; *AIMETA '01, XV Congresso Nazionale*, Taormina, 26-29 settembre 2001; Sommari, SS_DAN_12 (testo completo su CD Rom).
- [13] Vizzini A. J., Lagace P. A.: The buckling of a delaminated sublaminar on an elastic foundation, *J. of Composite Materials*, Vol. 21, pp. 1106-1117 (1987).
- [14] Bruno D., Grimaldi A.: Delamination failure of layered composite plates loaded in compression, *Int. J. of Solids and Structures*, Vol. 26, pp. 313-330 (1990).
- [15] Corigliano A.: Formulation, identification and use of interface models in the numerical analysis of composite delamination, *Int. J. of Solids and Structures*, Vol. 30, pp. 2779-2811 (1993).
- [16] Point N., Sacco E.: A delamination model for laminated composites, *Int. J. of Solids and Structures*, Vol. 33, pp. 483-509 (1996).
- [17] Kardomateas G. A., Pelegri A. A., Malik B.: Growth of internal delaminations under cyclic compression in composite plates, *J. of the Mechanics and Physics of Solids*, Vol. 43, pp. 847-868 (1995).